View metadata, citation and similar papers at core.ac.uk
brought to you by CORE
provided by DCU Online Research Access Service

Effect of Polycrystallinity on the Optical Properties of Highly Oriented ZnO Grown by Pulsed Laser Deposition

E. McGlynn[1], J. Fryar[1], G. Tobin[1], C. Roy[1], M.O. Henry[1], J-P. Mosnier[1], E. de Posada[2], J.G. Lunney[2]

[1]*School of Physical Sciences/NCPST, Dublin City University, Glasnevin, Dublin 9, Ireland.*

[2]*Dept. of Pure & Applied Physics, Trinity College, Dublin 2, Ireland.*

We report the results of photoluminescence and reflectance measurements on highly c-axis oriented polycrystalline ZnO grown by pulsed laser deposition. The samples measured were grown under identical conditions and were annealed in-situ at various temperatures for 10-15 minutes. The band-edge photoluminescence spectra of the material altered considerably with an increase in grain size, with increased free exciton emission and observable excitonic structure in the reflectance spectra. The green band emission also increased with increasing grain size. A deformation potential analysis of the effect of strain on the exciton energy positions of the A- & B-excitons demonstrated that the experimental exciton energies couldn't be explained solely in terms of sample strain. We propose that electric fields in the samples due to charge trapping at grain boundaries are responsible for the additional perturbation of the excitons. This

interpretation is supported by theoretical estimates of the exciton energy perturbation due to electric fields. The behaviour of the green band in the samples provides additional evidence in favour of our model.

PACS Numbers: 81.15.Fg, 78.40.Fy, 78.55.Et, 78.66.Hf, 68.55.Jk, 68.60.Dv

Keywords: Pulsed laser deposition, Zinc oxide, Optical properties, Annealing.

Author to whom correspondence should be addressed: enda.mcglynn@dcu.ie

I: Introduction

ZnO is receiving a great deal of attention recently as a candidate material for short wavelength emitters, in particular due to its large exciton binding energy and the availability of lattice matched substrates which give it substantial advantages over GaN-based devices [1-3].

Most of the recent research on ZnO has concentrated on epitaxial growth of thin films and their properties, and device production was the driving motivation in many cases [4, 5]. Many of the samples (grown by a range of methods) were polycrystalline. Understanding the effects of the polycrystalline nature of the samples on their properties is thus important.

In this report, photoluminescence (PL) and reflectance spectroscopy were employed to characterise ZnO thin films grown using pulsed laser deposition (PLD). This technique has been previously shown to produce high quality ZnO thin films, with excellent electronic and optical properties [6, 7]. The samples were annealed in situ at different temperatures immediately after deposition. The PL and reflectance data were compared with corresponding data from a bulk single crystal.

II: Experimental Details

A ceramic polycrystalline ZnO target (99.99 %) and a KrF excimer laser (λ = 248 nm) with laser energy density of 1.7 J/cm^2 at a pulsed repetition rate of 10 Hz and pulse duration of 26 ns were used for the ablation process. The target to substrate distance was ~ 4 cm. The ZnO films were deposited on (0001) sapphire substrates at an oxygen (99.99 %) pressure of 30 Pa (0.3 mbar) and the substrate temperature was maintained at 400 °C during growth. Typically the films were 150-200 nm thick, giving a deposition rate of 0.025 nm/pulse. Some samples were further annealed in O_2 (30 Pa) at temperatures of 400 °C and 500 °C respectively (Table I) in the growth chamber immediately after deposition. The anneals at 400 ^{o}C and 500 °C are not isochronal, and thus we cannot separate the effects of increased anneal time and temperature. They are sufficient however for the purposes of this work, in that the overall annealing effect will definitely be greater e.g. in sample (iii) than in sample (ii) as sample (iii) has been exposed to a higher temperature for a longer time period. The single crystal material was obtained from the Eagle Picher corporation.

The 325 nm line of a continuous wave HeCd laser (output ~40 mW unfocussed on the sample) provided PL excitation. The emission from the sample was analyzed using a 1 metre grating spectrometer and detected with a photomultiplier tube operated in photon counting mode. Controllable temperatures from 10 K to 300 K were achieved using a closed cycle cryostat. The typical spectral resolution of the PL data was ~0.25 meV and 0.1 meV for the data presented in figure1 and figures 2 & 4 respectively.

Reflectance measurements were performed using a Fourier-transform (FT) spectrometer fitted with a photomultiplier tube. Samples were studied at temperatures between 20 and 300 K using a closed-cycle cryostat. A 150 W Xe-arc lamp was used to illuminate the samples at an incident angle of approximately 45 degrees, after beam confinement through a variable aperture. No focusing was used and the incident light was unpolarised. Although this configuration was sufficient for the examination of the general reflectance characteristics of the samples, the oblique angle of incidence and unpolarised nature of the incident light does not readily allow a detailed analysis of exciton-polariton features. Since the spectral region of interest is in the UV, and to avoid saturation of the detector (due to the multiplex nature of the FT spectrometer data acquisition), visible wavelengths were removed from the reflected beam with an appropriate glass filter. As a reference, we used a silicon sample onto which a thick layer of aluminium was deposited. Typical reflectivity for this reference sample is approximately 93 %. The typical spectral resolution of the reflectance data was ~0.5 meV.

III: Results

Previous measurements on these samples using x-ray diffraction along with Raman spectroscopy data [8] show that these samples are polycrystalline and the grain structure is columnar with c-axis orientation. Significant electric field effects (due to charge trapping at the grain boundaries) are seen. The grain sizes (parallel to the growth direction) determined from x-ray measurements are given in table I. AFM measurements

of lateral grain size confirm the x-ray results and also clearly show the increase in grain size with anneal. The surface roughness (taken as the standard deviation of the AFM tip height across a 2 μm profile) of the samples was also seen to decrease with increasing grain size from a value of > 10 nm down to ~ 3 nm for the sample annealed at 500 ^{0}C.

Figure 1 shows PL spectra at 20 K and 300 K for the three PLD grown samples. These spectra show that all the samples have strong band-edge, UV emission and with varying amounts of green band emission. Other workers have found similar results for ZnO materials grown using PLD [9]. The bound exciton (BE) luminescence in the case of the PLD samples is substantially broadened, and the individual lines seen in the bulk material cannot be resolved in the PLD material. The width of the BE feature in PLD material is ~12 meV compared to the bulk crystal value for a single line of ~1 meV. We note that the room temperature peak PL intensities for all three samples are quite similar, with the unannealed sample actually having the highest peak intensity. The room temperature integrated intensities across the entire spectral range of the annealed samples are slightly higher than that of the unannealed samples. At low temperatures however, we see that the peak and integrated intensity of the unannealed sample is substantially lower than the annealed samples. The integrated intensities of the two annealed samples are quite similar at low temperature. One must be careful in making sample to sample comparisons of PL intensities due to the variations that may occur in alignment etc., however there is a very definite increase in low temperature PL intensity from the unannealed sample to the two annealed samples. We also note a relative increase in the intensity of the green band (~ 2.4 eV) compared to the band-edge emission with increased annealing, and the

appearance of a structured luminescence below the BE emission in the two annealed samples which is not present in the unannealed sample.

In figure 2 we compare PL and reflectance data for the three PLD grown samples at 20 K and for the bulk crystal at 50 K (temperature for the bulk sample was chosen to show LO phonons replicas more strongly) in the near band-edge region of the spectrum. For all samples, as noted above, we see strong BE luminescence in the region around 3.360 eV. In the bulk crystal we observe longitudinal optic (LO) phonon replicas of both the A and B free excitons (FE), with some evidence (from the PL temperature dependance) of zero-phonon luminescence from the A exciton above the BE lines.

IV: Discussion / Analysis of Results

In the case of the PLD samples, we note that all samples show strong BE PL. For the unannealed sample the higher energy peak on the shoulder of the main PL line (Figure 2(a)) is likely to be due to surface excitons, reported in [10], which is expected for samples with small grain size and consequently large "surface-like" character of the material. For the two annealed samples (figure 2(b,c)), we see a substantial change in the band-edge PL. We note the appearance of broad lines below the main PL line at energies of 3.330 eV and 3.255 eV with a separation of ~ 75 meV which corresponds closely to the LO phonon energy of 72 meV [11]. We attribute these PL features to the LO phonon replicas of the B exciton. This assignment is supported by an increase in the ratio of LO to 2LO emission intensities with increasing temperature in these samples as expected for

the ratio between the first and second phonon replicas of a free exciton complex [12]. A recent report in the literature has also described similar PL features, and have assigned these features to an acceptor bound exciton [13]. However, the large concentration of impurities at the growth interface in the sample reported in [13] may be the origin of significant polycrystallinity which might provide an alternative explanation (as discussed below) of the feature they observe, consistent with our assignment. We also see some evidence for the 1-LO replica of the A exciton at ~3.306 eV, but it is weak in comparison to the FE(B)-LO replicas. These assignments are further supported by the relative sizes of the A- and B-exciton features in the reflectance data. Thus with increased annealing we see a substantial and consistent growth in the contribution of FE phonon replicas to the PL, compared to the BE luminescence. This increase in FE luminescence may be expected due to the reduction in the point and extended defect density as the grain size increases [8].

Reflectance data has been widely published for bulk ZnO [14,15], but, to the best of our knowledge, there are few reports on polycrystalline material such as the PLD samples we have examined. The reflectance data for the bulk crystal shows similar form to those published earlier [14], with A-, B- and C-exciton features at ~ 3.361 eV, 3.391 eV and 3.428 eV respectively. Comparing the PL and reflectance spectra for the bulk sample (Figure 2(d)) leads to the identification of PL lines with LO replicas of both FE(A) and FE(B) recombination. Although reflectance data on the PLD samples is substantially distorted we see clear resonances in samples (i), (ii) and (iii), at ~ 3.374 eV and 3.390 eV. The energy difference between the 3.390 eV reflectance resonance and the 3.330 eV PL

line in these two samples matches the LO phonon energy of 72 meV (with the difference explained by the difficulty in locating the lower energy "cut-on" for the LO phonon replica with such broad lineshapes), and this supports our previous assignment of the 3.330 eV PL line to FE(B)-LO emission.

We now consider the details of the reflectance from the A-and B- excitons in the PLD samples compared to the bulk sample at 20 K. The excitonic reflectance anomalies are substantially damped compared to the bulk crystal, particularly for the unannealed sample, where the reflectance signatures are extremely weak. These features recover in both the annealed samples. A significant strain exists in all the PLD-grown samples, as previously measured by XRD [8]. The c-axis lattice parameters for all the PLD-grown samples are 0.518 nm and the values for all samples were identical within the limits of our experimental accuracy. The samples are under tensile biaxial strain following deposition on the (0001) sapphire substrate with strain values of $e_{zz} = -6 \pm 1 \times 10^{-3}$. We have plotted in figure 3 the variation of the A-, B- and C- transverse exciton energies with tensile biaxial strain using the deformation potential Hamiltonian in [16, 17] and the fit parameters in these papers, with the small exchange interaction term set to zero. We have superimposed on this the positions of the A- , B- and C excitons from the bulk crystal, at zero strain, and the positions of the A- and B-excitons from the PLD samples, all taken at 20 K. The position in energy (from figure 2) of the reflectance minimum is taken as the longitudinal exciton energy [15] and the positions of the B- and C- excitons are corrected by the longitudinal-transverse splittings (~10 meV) [16] to give the transverse exciton position. We note that our estimation of the transverse exciton energies

in the PLD samples will have an error of ~ ± 2. 5 meV for the B-exciton and ~ ± 1 meV for the A-exciton due to the rather broad excitonic reflectance anomalies in the PLD samples compared to the bulk. Additionally, we have neglected any possible changes in the longitudinal-transverse splittings in the PLD samples compared to the bulk. Work is in progress to study this problem in more detail using a two band exciton-polariton model.

One can immediately note that the bulk crystal exciton energies are well described by the model Hamiltonian and the fit parameters from [16, 17]. The exciton energies for the PLD samples however are different to those predicted by the model. For the unannealed sample the energy difference for the A-exciton is +9 meV and +25 meV for the B-exciton. This reduces in the annealed samples to +6 meV and +8 meV respectively for the sample annealed at 400 ^{0}C and to +6 meV and +11 meV respectively for the sample annealed at 500 ^{0}C. The energy differences for the two annealed samples are identical within the experimental error, but there is a very substantial reduction compared to the unannealed sample. The energy differences are positive in all cases, indicating that the actual energy positions are higher than those expected purely on the basis of strain effects. Additionally, the energy difference for the B-exciton is in all cases larger than that of the A-exciton.

We conclude that there must be additional perturbing effects on the exciton energies in these samples. As mentioned in section II above, x-ray diffraction and Raman spectroscopic measurements on the PLD-grown samples show an oriented columnar

polycrystalline grain structure with the grains highly oriented along the c-axis, and a continuous increase in the polycrystalline grain size with increased annealing [8]. Raman data in particular have shown evidence for electric fields due to depletion layers formed by charge trapping at grain boundaries, which decreased as the grain size increased. We propose that the additional perturbation experienced by the excitons is caused by the same effect. This explains the reduced perturbation observed in the samples annealed at 400 ^{o}C and 500 ^{o}C, as these samples have larger grain sizes (table I) and hence reduced grain boundary density and electric field effects. The sample annealed at 500 ^{0}C actually has the same A-exciton energy difference as the sample annealed at 400 ^{0}C, and a slightly larger B-exciton energy difference. However, considering that the grain size in the two annealed samples is quite similar and given the rather large error associated with the transverse energy estimation (particularly for the B-exciton) as mentioned above, we feel that more detailed work on modelling the reflectance lineshapes using a polariton model will be needed to correctly assignment transverse exciton energy differences between these two samples for a meaningful comparison.

Our interpretation of the origin of exciton energy shifts in the PLD samples is in good agreement with theoretical descriptions of the effect of electric fields on exciton energies [18, 19]. In reference 18, a universal curve relating the change in exciton energy to the electric field in the sample is given (as a multiple of the ionisation field, corresponding to a potential drop of 1 Rydberg across the exciton Bohr radius, when substantial exciton ionisation begins). For electric fields equal to or greater than the ionisation field the exciton energy difference compared to the zero field case is always positive, in agreement

with our data. For ZnO the exciton energy difference due to such an electric field will have values of the order of ~ 6 meV and greater, again in general agreement with the order of magnitudes in our data.

Visual inspection of the reflectance anomalies shows that there is certainly substantial exciton damping for both A- and B-excitons, which is known to occur for electric fields greater than or equal to the ionisation field [19]. However we can make an independent check of the rough magnitude of the electric field and the ZnO ionisation field as follows. The ionisation field of a wide variety of semiconductors scales linearly with the exciton binding energy [18]. If we extrapolate using the values in reference 18 and the 60 meV binding energy for the exciton in ZnO [1] we find that the ionisation field for ZnO is ~ 300 x 10^3 V/cm. We may estimate the electric fields in the depletion regions at the grain boundaries using a simple model, similar to that used to determine depletion layer widths in p-n junctions [20]. The residual n-type carrier density in ZnO films grown by PLD on sapphire is generally in the range > 5 x 10^{17} cm^{-3} [6, 9] and the typical potential barriers between grains, associated with these depletion regions, is ~ 0.5 eV [21]. Using these figures and the static dielectric constant of ZnO [19], we can estimate that the electric fields in the depletion layers will be ~ 400 x 10^3 V/cm. Thus we are confident that the electric fields in our samples have values equal to or greater than the ionisation field for the excitons and that the consequent energy perturbations and damping predicted by theory are fully consistent with our data. In addition, this model predicts that a greater energy perturbation is associated with a stronger electric field and consequently greater exciton damping. We have seen that the energy difference for the B-exciton is in all cases

larger than that of the A-exciton. Preliminary fits to the reflectance data using a polariton model indicate that the B-exciton damping parameter needed to reproduce the data is significantly greater than the A-exciton damping parameter, in agreement with the theoretical predictions above.

PL data over a wider energy range for the three PLD samples is shown in figure 4. We see a clear trend in the data: the green band intensity increases relative to the BE intensity with increased annealing. The relative strength of the green luminescence in comparison to the band-edge PL is often taken as a measure of the sample quality, with strong green luminescence indicating lower quality. The data presented above and our earlier work [8] indicates a general reduction in defect density with increased annealing, in apparent contradiction with the PL results of figure 4. We can explain these data in a manner consistent with the interpretation above using the model proposed by Vanhuesden *et al.* [22]. In this model, the green band is attributed to transitions at a singly charged oxygen vacancy (V^{+}_{O}). At grain boundaries, where band-bending effects are substantial due to trapped charges, as mentioned above, these vacancies become doubly ionised (V^{++}_{O}) and the green luminescence is quenched. Our data are consistent with this model as the increase in grain size with annealing causes a reduction in the grain boundary density and hence the fraction of V^{++}_{O} compared to V^{+}_{O}. This results in an increase in the green luminescence band intensity with increasing grain size. This interpretation is also consistent with the results previously obtained by de Posada *et al.* [23].

V: Conclusion

We have performed PL and reflectance measurements on bulk and polycrystalline ZnO material, grown by PLD, with particular attention on the excitonic properties of the samples and the changes in these properties with annealing for the PLD samples. Our data show a consistent increase of material quality, in terms of PL band-edge emission intensity, linewidth and excitonic reflectance features, with increased annealing, though they still fall far short of the bulk crystal material, with excitonic linewidths approximately an order of magnitude larger. The PL spectra of the material show an increase in FE LO phonon-assisted signal with increased annealing. The reflectance data show similar trends, and assignments are made for the A- and B-exciton features on the reflectance spectra. Substantial shifts and quenching of the A- and B-excitons is observed and a possible origin due to electric field effects is presented and compared with theoretical estimates from the literature.

We also see a consistent increase in the intensity of the green luminescence band with increased annealing and explain this in terms of a previously reported model based on oxygen vacancies ionised due to electric fields, consistent with the interpretation of our band-edge data.

Acknowledgements

The authors wish to acknowledge financial support provided by the Enterprise Ireland Basic Research Grants programme, and the financial support of the Higher Education Authority through the PRTLI programme.

References

[1] D.C. Look, Mat. Sci. & Eng. B80, 383 (2001).

[2] G. Heiland, E. Mollwo, F. Stockmann, Solid State Phys. 8, 191 (1959).

[3] Y. Chen, D. Bagnall, T. Yao, Mat. Sci. & Eng. B75, 190 (2000).

[4] X. Guo, J. Choi, H. Tabata, T. Kawai, Jpn. J. Appl. Phys. 40, L177 (2001).

[5] D.M. Bagnall, Y.F. Chen, Z. Zhu, T. Yao, S. Koyama, M.Y. Shen, T. Goto, Appl. Phys. Lett. 70, 2230 (1997).

[6] A. Ohtomo, K. Tamura, K. Saikusa, K. Takahashi, T. Makino, Y. Segawa, H. Koinuma, M. Kawasaki, Appl. Phys. Lett. 75, 2635 (1999).

[7] T. Makino, G. Isoya, Y. Segawa, C.H. Chia, T. Yasuda, M. Kawasaki, A. Ohtomo, K. Tamura, H. Koinuma, J. Cryst. Growth 214/215, 289 (2000).

[8] C. Roy, S. Byrne, E. McGlynn, J-P Mosnier, E. de Posada, D. O'Mahony, J. G. Lunney, M. Henry, B. Ryan, A.A. Cafolla, Thin Solid Films 436, 273 (2003).

[9] B.J. Jin, S. Im, S.Y. Lee, Thin Solid Films 366, 107 (2000).

[10] S. Savikhin, A.Freiberg, J. Lumin. 55, 1 (1993).

[11] R.L. Weiherr, W.C. Tait, Phys. Rev. 166, 791 (1968).

[12] C. Klingshirn, Phys. Stat. Sol. (b) 71, 547 (1975).

[13] D.C.Look, D.C. Reynolds, C.W. Litton, R.L. Jones, D.B. Eason, G. Cantwell, Appl. Phys. Lett. 81, 1830 (2002).

[14] D.C. Reynolds, D.C. Look, B. Jogai, R.L. Jones, C.W. Litton, W. Harsch, G. Cantwell, J. Lumin. 82, 173 (1999).

[15] J.J. Hopfield, D.G. Thomas, Phys. Rev. Lett. 15, 22 (1965).

[16] B. Gil, A. Lusson, V. Sallet, S. Daid-Hassani, R. Triboulet, P. Bigenwald, Jpn. J. Appl. Phys. 40, L1089 (2001).

[17] J. Wrzesinski, D. Frohlich, Phys. Rev. B56, 13087 (1997).

[18] D.F. Blossey, Phys. Rev. B3, 1382 (1971).

[19] J. Lagois, Phys. Rev. B23, 5511 (1981).

[20] J. Singh, Semiconductor Devices (2001, Wiley, New York).

[21] T. L. Tansley, D. F. Neely, C. P. Foley, Thin Solid Films 117, 19 (1984).

[22] K. Vanheusden, W.L. Warren, C.H. Seager, D.R. Tallant, J.A. Voight, B.E. Gnade, J. Appl. Phys. 79, 7983 (1996).

[23] E. de Posada, G. Tobin, E. McGlynn, J.G. Lunney, Appl. Surf. Sci., 208-209, 589 (2003).

Tables

Table I: Various parameters of the annealed PLD-grown ZnO thin films.

Sample	Annealing temp. (^{o}C)	Annealing time (min)	Average grain size (nm) [8]
(i)	No anneal	0	32
(ii)	400	10	67
(iii)	500	15	79

Figure Captions

Figure 1:

PL data for the three PLD samples at 20 K and 300 K. Multipliers given allow comparison of the three sample intensities at the same temperature, but do not relate the 300 K measurements to the 20 K measurements.

Figure 2:

PL and reflectance data for the three PLD samples at 20 K and the bulk material at 50 K. Positions of FE and LO phonon replicas are indicated for sample (ii) and the bulk crystal, with similar assignments for samples (i) and (iii). All linewidths are sample limited.

Figure 3:

Plot of variation of exciton energy with strain. The continuous lines are the prediction based on the deformation potential model. The various other points show the position of the A- and B-excitons for the PLD samples and the bulk sample. For each PLD sample the lower and higher energy data points are the A-exciton and B-exciton transverse energies respectively. The errors in the exciton energy for the PLD samples are ~ 2 meV for the A-exciton and ~5 meV for the B-exciton. The error for the bulk sample is smaller than the data point size.

Figure 4:

PL data for the three PLD samples at 20 K. The samples are normalised so that the BE peak intensity is the same in all three graphs.

Figure 1

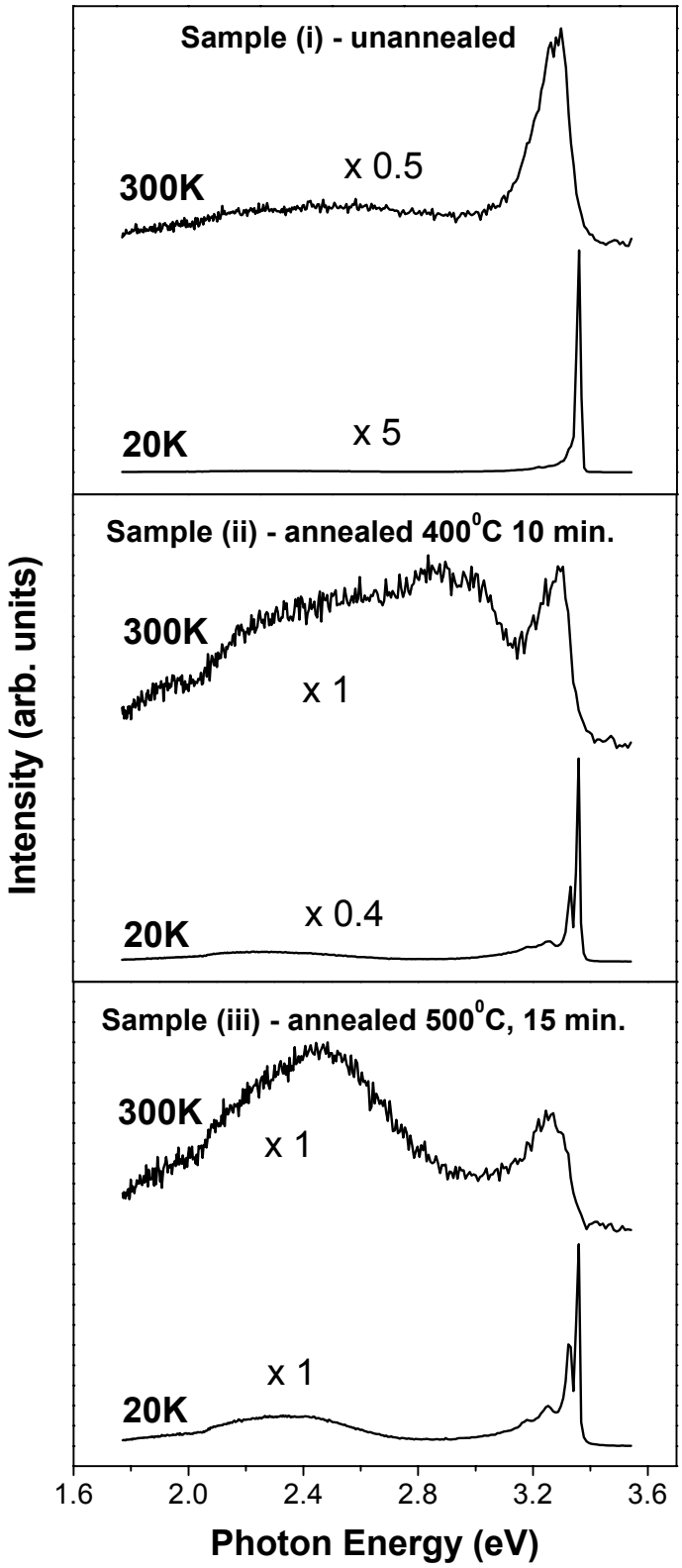
Sample (i) - unannealed
300K
x 0.5
20K
x 5
Sample (ii) - annealed 400°C 10 min.
300K
x 1
20K
x 0.4
Sample (iii) - annealed 500°C, 15 min.
300K
x 1
20K
x 1
Intensity (arb. units)
1.6
2.0
2.4
2.8
3.2
3.6
Photon Energy (eV)

Figure 2

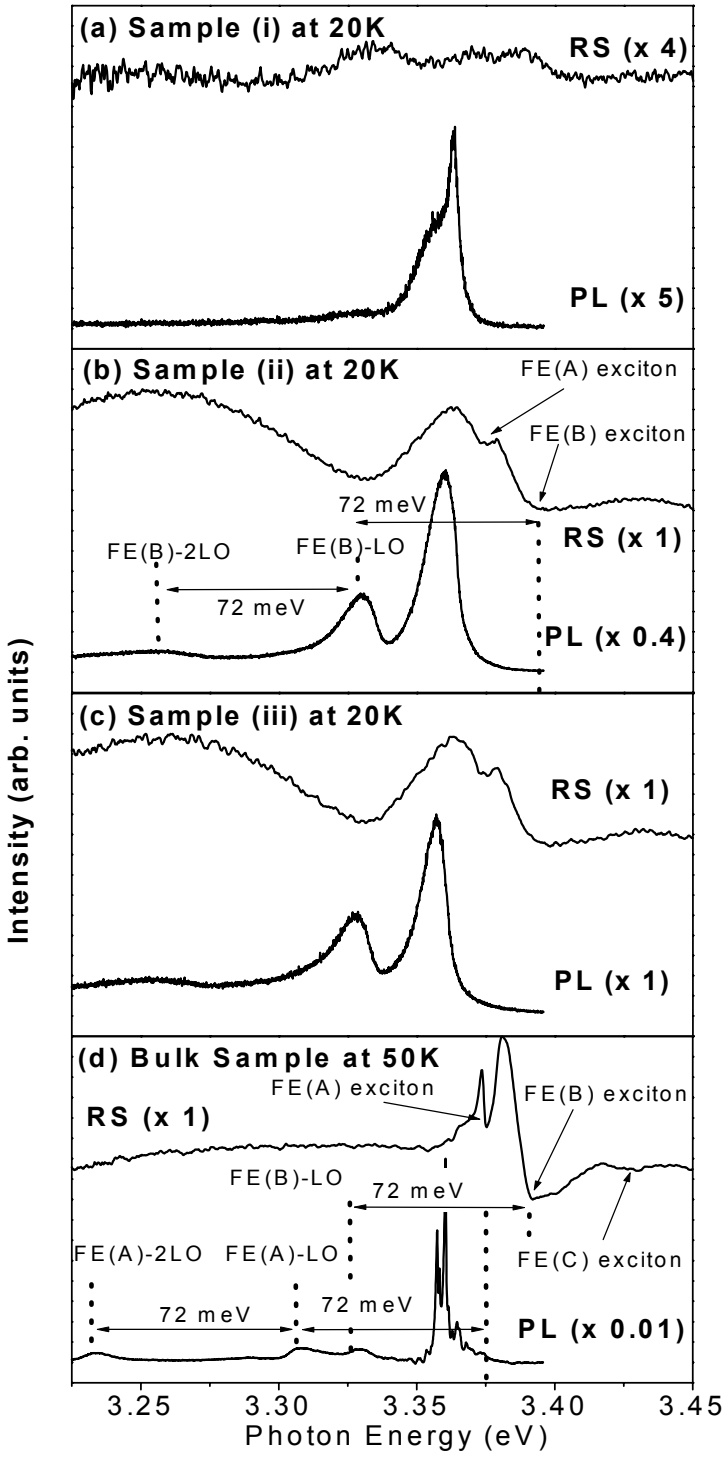
(a) Sample (i) at 20K
RS (x 4)
PL (x 5)
(b) Sample (ii) at 20K
FE(A) exciton
FE(B) exciton
72 meV
RS (x 1)
FE(B)-2LO
FE(B)-LO
72 meV
PL (x 0.4)
(c) Sample (iii) at 20K
RS (x 1)
PL (x 1)
(d) Bulk Sample at 50K
FE(A) exciton
FE(B) exciton
RS (x 1)
FE(B)-LO
72 meV
FE(A)-2LO
FE(A)-LO
FE(C) exciton
72 meV
72 meV
PL (x 0.01)
Intensity (arb. units)
3.25
3.30
3.35
3.40
3.45
Photon Energy (eV)

Figure 3

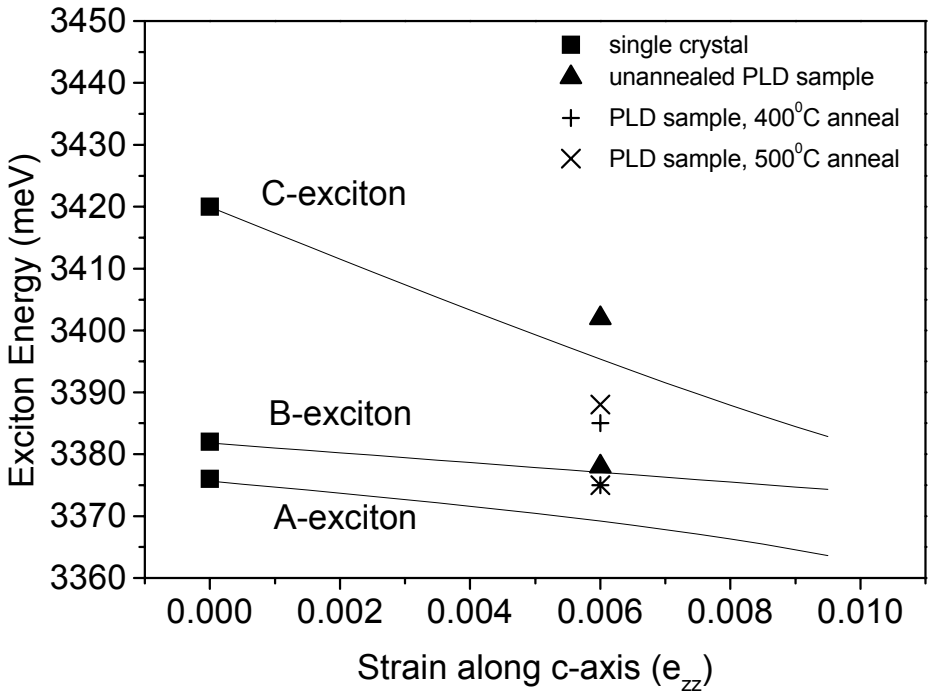
3450
3440
3430
3420
3410
3400
3390
3380
3370
3360
Exciton Energy (meV)
0.000
0.002
0.004
0.006
0.008
0.010
Strain along c-axis (e_zz)
single crystal
unannealed PLD sample
PLD sample, 400°C anneal
PLD sample, 500°C anneal
C-exciton
B-exciton
A-exciton

Figure 4

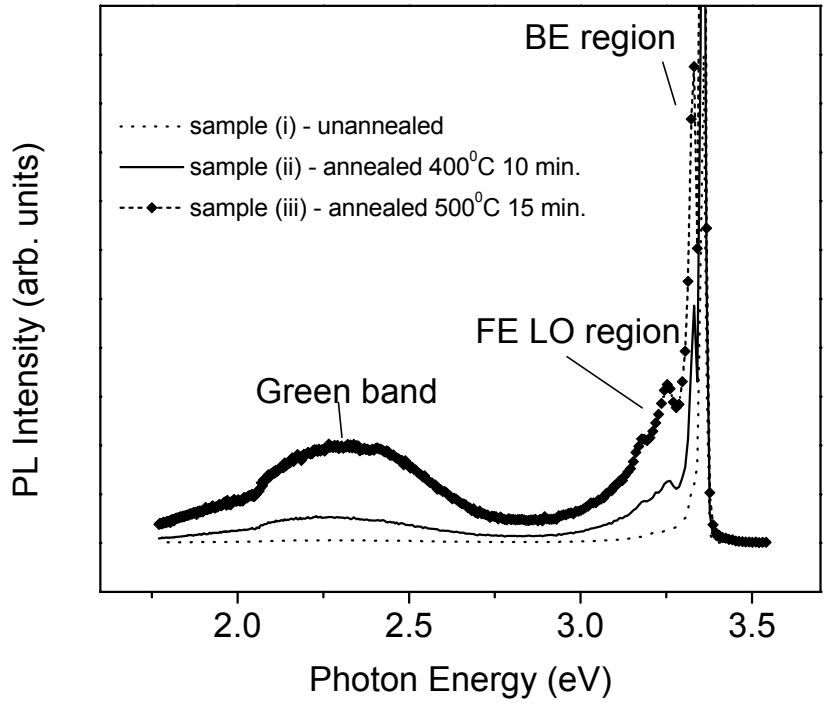
BE region
sample (i) - unannealed
sample (ii) - annealed 400^{0}C 10 min.
sample (iii) - annealed 500^{0}C 15 min.
FE LO region
Green band
PL Intensity (arb. units)
2.0
2.5
3.0
3.5
Photon Energy (eV)